Boslough, M.B., Crawford, D.A., Trucano, T.G., and Robinson, A.C. (1995) Numerical modeling of Shoemaker-Levy 9 impacts as a framework for interpreting observations, **Geophys. Res. Lett. 22**, 1821-1824.

Numerical modeling of Shoemaker-Levy 9 impacts as a framework for interpreting observations

Mark B. Boslough, David A. Crawford, Timothy G. Trucano, and Allen C. Robinson

Sandia National Laboratories, Albuquerque, New Mexico

Abstract. Computational models of the impacts of Comet Shoemaker-Levy 9 onto Jupiter may provide the best framework by which the observational data can be interpreted. Among the observations that have already been at least partially explained in a way that appears to be consistent with the impact models are: the sources and timings of multiple flashes observed from Earth, the temperatures and durations of the single flashes observed from the Galileo spacecraft, and the asymmetry of the plumes and ejecta patterns observed by the Hubble Space Telescope. Further modeling subsequent to the impacts has shown that (contrary to our pre-impact expectations) fireball trajectory data do not provide strong constraints on either fragment mass or maximum penetration depth. Instead, it is the cross-sectional area of the fragment (or swarm of sub-fragments) at the time of impact that determines the ejection velocity and trajectory of the fireball. The observation of seemingly consistent plume heights, coupled with this computational result, suggests that SL-9 fragments were loosely-bound "rubble piles," possibly with widely varying masses, that in most cases dispersed to about the same diameter (2.0 ± 0.5 km) by the time they reached the Jovian atmosphere. After more data become available and correlated, and more simulations are performed, we expect that fragment size estimates will become more precise.

Introduction

The impacts of Comet Shoemaker-Levy 9 (SL-9) fragments in July, 1994, provided an historic opportunity to directly observe the phenomena resulting from hypervelocity collisions on a planet. Detailed analysis of this event will improve our understanding of comets, of Jupiter, and of the collisional processes that shaped the solar system. Because of the massive international effort, an overwhelming amount of high-quality observational data has been collected. To help provide a framework for interpretation of this data, we have continued our computational effort with emphasis on observable phenomena. A reasonably consistent picture has already begun to emerge.

Prior to impact, there was general agreement among the impact modeling groups that, for sufficiently large impactors, debris ejected by the collisions would rise into line of sight of Earth [*Zahnle & Mac Low*, 1994; *Stellingwerf et al.*, 1994; *Ahrens et al.*, 1994; *Boslough et al.*, 1994a,b; *Shoemaker et al.*, 1995]. The fireballs and plumes predicted by the models were indeed observed, but the actual event produced a much richer array of consequences than anyone anticipated. Some of these new phenomena have already been explained and are fully consistent with the models. Interpretation of other observations will require further analysis and synthesis of the data. We expect that computational modeling will continue to provide guidance and contribute to our understanding of this event. In this paper, we attempt to provide a "big picture" interpretation that is consistent with much of the observa-

tional data that has become available to date (see other papers in this volume; and *Science, 267*, March 3, 1995), and to present the results of some post-impact simulations that have provided further insight into the aftereffects of the impact of Shoemaker-Levy 9 on Jupiter. We present the conceptual framework both as a guide for data interpretation and for determination of future directions for computational work.

Bolides, Fireballs, and Plumes

Pre-impact computational simulations suggested fireballs as the most likely effect observable from Earth during the first few minutes after impact. Analysis of the simulations in relation to the predicted viewing geometry led to the conclusion that the ballistic trajectories of the fireballs could be determined from time-resolved observational data, and that useful information about the impactors could be extracted from these trajectories [*Boslough et al.*, 1994a,b; *Crawford et al.*, 1994, 1995].

For the purposes of the present paper, the term "fireball" refers to the mass of hot gases consisting of a mixture of Jovian atmosphere and cometary material that is ballistically shot upward by the impact. In the first moments after impact it is very hot, incandescent, and radiating in the visible and near infrared. The fireball is preceded by the "entry flash" or "bolide" phase, during which time the comet fragment deposits its energy in the column of atmosphere that then radiates at high temperature. It is that column of gas that explosively expands and becomes the fireball. We use the word "plume" to describe the debris bubble after it has expanded, cooled adiabatically, and begun to condense. Clearly, there are no precise temporal demarcations separating bolide, fireball, and plume phases.

Interpretations

Figures 1 and 2 depict idealized schematic representations of the sequence of events inferred from Earth-based photometry data, Galileo light curves, and HST imagery. Figure 1 is a plan view of the impact site from a stationary (non-rotating) vantage point, with snapshots of a map projection of the evolving impact sites at various time intervals after impact. As the point of impact rotates from west to east, it moves from left to right in the stationary field of view of the illustration. Jovian north is up; the approximately vertical lines represent the minimum line-of-sight altitudes to the Earth and sun. The figure is not intended to depict the exact geometry, nor is it supposed to represent a particular impact, but is a composite of features observed from various events. Figure 2 shows a simplified side view of the fireball/plume evolution. In reality, the ejecta cloud is not a discrete packet but a continuum with widely varying temperatures, densities, and pressures. In addition, the impacts were not necessarily the "clean experiments" described here, but probably involved closely-spaced multiple impactors embedded within a dusty, light-scattering cloud of smaller particles (coma), which also had a hypervelocity interaction with Jupiter's atmosphere.

In the Figure 1 inset are some idealized examples of Galileo and Earth-based light curves. The Galileo Photopolarimeter Radiometer (PPR) curve is based on the measurements of several impacts at 945 nm [*Martin et al.*, 1995]. The upper Earth-based light curve resembles data at 3.5 μm collected at the Palomar Observatory by

Nicholson et al. [1994] for the R impact; a similar curve was obtained by *Graham et al.* [1994] at 2.3 μm with the Keck Telescope. The lower curve is based on 10 μm data collected at the European Southern Observatory by *Livengood et al.* [1994].

The following is a description of the sequence of events, with letters corresponding to those in Figures 1 and 2. The various phases are defined primarily for conceptual purposes; there are not distinct demarcations between them, and in many cases they overlap. Approximate times relative to initial entry are listed for each.

(a) Entry phase (zero to 10 or 15 seconds)

A fragment (or cluster) enters Jupiter's atmosphere, depositing energy and leaving a debris column that consists of a mixture of Jovian atmosphere and cometary vapor at high temperatures and pressures. Thermal radiation from this column is seen directly by Galileo's instruments, and, for some impacts, via scattered light (or directly in the earliest stages) from Earth. This appears as the first precursor in some of the Earth-based light curves. The long rise-time associated with this precursor is probably due to the direct view from Earth of the hypervelocity collision of the leading part of the coma into Jupiter's upper atmosphere.

(b) Fireball phase (5 or 10 seconds to 3 or 4 minutes)

The column explosively expands upward and outward along the atmospheric density gradient, cooling isentropically as it rises. The expansion begins instantaneously, before the entry phase is complete. This is seen by Galileo as a decrease in radiative intensity, and a shift toward longer wavelengths in thermal emission. Within one minute, the incandescent fireball rises to a few hundred kilometers and becomes visible from Earth, appearing as another precursor in photometry data. The exact timing depends on both fragment size and the point of impact, as summarized by *Crawford et al.* [1995]. The fireball is preceded by several seconds by a shock wave. Earth-based detection of this shock would provide strong validation of the computational models, but it may be too weak to have been seen as an independent precursor. The arrival time of hot material above the Jovian limb, as viewed from Earth, is probably blurred by fireball light scattered from trailing coma material.

(c) Plume phase (3 or 4 minutes to 10 or 15 minutes)

The debris continues to rise ballistically. It expands and cools, and begins to condense. When it reaches an altitude greater that one or two thousand kilometers (depending on the point of impact), it enters sunlight. Careful analysis of time-resolved photometry might provide the timing for this event, which would be useful for constructing the ballistic trajectory.

(d) Maximum height (between about 6 and 9 minutes)

The lower part of the debris cloud begins to collapse and heat Jupiter's stratosphere. As the front of this heated region propagates and rotates over the limb, the strongest peak in the Earth-based light intensity curves begins to appear.

(e) Plume collapse phase (about 5 to 15 minutes).

As the still-expanding debris cloud begins to fall back, it compresses and heats a large area of the Jovian stratosphere. The heated region grows rapidly. The peak in Earth-based photometry curves is determined by a combination of competing effects, including increasing area, radiative and decompressional cooling, and viewing geometry. Recently-downloaded data on the R impact from Galileo's Near Infrared Mapping Spectrometer (NIMS) has now provided direct evidence for stratospheric heating from the collapse of the plume, and timing information for that event (Weissman, unpublished data, 1995). The expanding debris cloud rotates counterclockwise due to the Coriolis Effect, so the ejecta footprint's symmetry axis does not line up with the fragment trajectory. The outwardly-directed velocity component sets up a radially-expanding flow field that sweeps condensed matter outward.

(f) Post-collapse "splat" phase (about 15 to 45 minutes).

The plume collapse goes to completion. The fully-collapsed ejecta blanket continues to expand radially and rotate counterclockwise until stopped by viscous and other dissipative forces. The final angle between the impact trajectory and axis of bilateral symmetry depends on how much rotation takes place after the plume collapses. The post-collapse rotation is evidence that ejected material flows horizontally over very long distances after reentry, and indicates that the ejecta blanket also expanded radially. A linear, radially expanding wave is made visible by an unknown mechanism, possibly condensation in the rarefaction part of the wave.

(g) Upwelling phase (minutes to hours)

The computational models indicate that there is also an upwelling phase. Careful examination of the 3-D simulations of *Crawford et al.* [1995] reveals that for massive, deeply-penetrating impactors, a bubble (or several bubbles) of hot Jovian atmosphere mixed with cometary vapor rises buoyantly from the depth of maximum energy deposition. This is between 200 and 300 km beneath the 1 bar level for 2-3 km diameter fragments. At 82 seconds after impact for a 1-km impactor there are three or four instabilities developing between about 50 and 200 km below the 1 bar level. At this time, they are 20-30 km in diameter, and have risen by about that distance from their starting point. These bubbles are analogous to buoyant nuclear explosion fireballs. Extrapolation of their upward motion suggests that they will begin arriving at the ammonia cloud layer within minutes, after having adiabatically expanded to many times their size. The resulting massive displacement of atmosphere is a likely source for the expanding wave. The upwelling might also manifest itself as thermal brightening or appearance of new spectroscopic signatures at the impact sites. It may be possible to extract information about the penetration depth (and therefore fragment mass) from the timing, temperature, and composition of any buoyantly-upwelling material. High-resolution 3-D simulations of this buoyancy phase are clearly needed.

Simulations and Implications

Preliminary 3-D simulations of plume evolution following the impact of a 3-km diameter ice fragment provide support for many

of the interpretations presented in the previous section. Figure 3 shows that, over a period of about twenty minutes, the plume rises to its maximum height and collapses over a large area. In this simulation, the plume reaches an altitude nearly twice that observed for several plumes (including the G plume) by HST. When comparing the simulated with the observed plumes one must consider the fact that the observed plume height partially depends on the minimum density at which the debris cloud begins to condense and scatter sunlight. The diameter of the fallback region is about 30% larger than the dimensions of the G impact site. This suggests that the G fragment (or swarm of fragments) had a diameter of somewhat less than 3 km at the time of entry.

Computational simulations have now demonstrated that fireball evolution depends much more strongly on impactor diameter than on its mass. Figure 4 shows the results of a pair of 2-D simulations of early-time fireball growth after the impact of a 3-km diameter sphere of solid ice. In the left-hand simulation, the initial conditions included the entire energy deposition of the entry phase down to the maximum penetration depth of about 320 km below the 1 bar level. For the right-hand simulation, the energy deposition curve was truncated at a depth of 50 km, below which the entry column was replaced with undisturbed Jovian atmosphere. After a little over one minute, the fireballs are virtually identical. Examination of the energy-deposition profile that was used for this simulation (see Fig 4a, *Crawford et al.*, 1995), shows that only a fraction of a percent of the energy deposited by a solid 3-km diameter fragment would partition into fireball energy. *Crawford et al.* [1995] showed that a 3-km diameter solid ice sphere (0.95 g/cm^3) and a 3-km diameter porous ice sphere (0.30 g/cm^3) have almost identical energy deposition curves above about 50 km below the 1 bar level. This observation, coupled with the pair of simulations shown in Figure 4, implies that fireball growth depends more strongly on fragment diameter than on its mass. Moreover, whereas the maximum penetration depth depends strongly on fragment mass [*Crawford et al.*, 1995], this quantity cannot be determined only from fireball observations.

One of the most unexpected results of the Shoemaker-Levy 9 impact was that all the plumes observed in profile by HST seem to have reached the same altitude of about 3300 km [*Hammel et al.*, 1995]. This maximum plume height is independent of the pre-impact fragment brightness, and of the size and prominence of the post-impact ejecta blanket left in Jupiter's atmosphere. The plume-height observation implies that the fragments that generated them were all about the same diameter (roughly 2 km). The variation among impact sites suggests that the impactor masses (and densities) could have varied widely. This hypothesis is consistent with each impactor being an unconsolidated "rubble pile" as suggested by *Asphaug and Benz* [1994]. Unfortunately, fragment masses and penetration depths cannot be extracted directly from fireball observations, and will have to be inferred from other evidence.

Acknowledgments. This work was supported by the United States Department of Energy under Contract DE-AC04-94AL85000. This material is based upon activities supported by the National Science Foundation under Agreement No. 9322118. We are grateful to the many observational astronomers who quickly made their data available to the community.

References

Ahrens, T. J., T. Takata, J. D. O'Keefe, and G. S. Orton, Radiative signatures from impact of Comet Shoemaker-Levy 9 on Jupiter, *Geophys. Res. Lett., 21*, 1551-1553, 1994.

Asphaug, E. and W. Benz, Density of comet Shoemaker-Levy 9 deduced by modelling breakup of the parent 'rubble pile', *Nature, 370*, 120-124, 1994.

Boslough, M. B., D. A Crawford, A. C. Robinson, and T. G. Trucano, Mass and penetration depth of Shoemaker-Levy 9 fragments from time-resolved photometry, *Geophys. Res. Lett., 21*, 1555-1558, 1994a.

Boslough, M. B., D. A Crawford, A. C. Robinson, and T. G. Trucano, Watching for fireballs on Jupiter, *EOS, 75*, 305-310, 1994b.

Carlson, R. W. and the NIMS Science Team, Galileo infrared observations of the Shoemaker-Levy 9 G impact fireball: a preliminary report, *Geophys. Res. Lett.*, in press.

Crawford, D. A., M. B. Boslough, T. G. Trucano, and A. C. Robinson, The impact of comet Shoemaker-Levy 9 on Jupiter, *Shock Waves, 4*, 47-50, 1994.

Crawford, D. A., M. B. Boslough, T. G. Trucano, and A. C. Robinson, The impact of periodic comet Shoemaker-Levy 9 on Jupiter, *Int. J. Impact. Engng.*, in press.

Graham, J. R., I. de Pater, J. G. Jernigan, M. C. Liu, and M. E. Brown, The fragment R collision: W. M. Keck Telescope observations of SL9, *Science*, 267, 1320-1323.

Hammel, H. B., R. F. Beebe, A. P. Ingersoll, and 14 others, HST imaging of atmospheric phenomena created by the impact of Comet Shoemaker-Levy 9, *Science*, 267, 1288-1296.

Martin, T. Z., G. S. Orton, L. D. Travis, L. K. Tamppari, and I. Claypool, Observation of Shoemaker-Levy Impacts by the Galileo Photopolarimeter Radiometer, *Science*, in press.

Livengood, T. A., G. Bjoraker, T. Kostiuk, and 6 others, *Bull. Am. astr. Soc.*, 26, supplement.

Nicholson, P. D., P. Gierasch, J. Goodman, and 11 others, *Bull. Am. astr. Soc.*, 26, supplement.

Shoemaker, E. M., P. J. Hassig, and D. J. Roddy, Numerical simulations of the Shoemaker-Levy 9 impact plumes and clouds: a progress report, *Geophys. Res. Lett.*, in press.

Stellingwerf, R. F., N. M. Hoffman, and C. A. Wingate, *Bull. Am. astr. Soc., 26*, 880, 1994.

Zahnle, K. and M.-M. Mac Low, The collision of Jupiter and Comet Shoemaker-Levy-9, *Icarus, 108*, 1-17, 1994.

M. B. Boslough, D. A. Crawford, T. G. Trucano, and A. C. Robinson, Experimental Impact Physics and Computational Physics Research and Development Depts., Sandia National Laboratories, MS 0821, Albuquerque, NM 87185-0821. (e-mail: mbboslo@sandia.gov)

(Received: February 21, 1995; revised: May 15, 1995; Accepted: June 5, 1995.)

BOSLOUGH ET AL.: NUMERICAL MODELING OF SHOEMAKER-LEVY 9 FRAGMENTS

BOSLOUGH ET AL.: NUMERICAL MODELING OF SHOEMAKER-LEVY 9 FRAGMENTS

BOSLOUGH ET AL.: NUMERICAL MODELING OF SHOEMAKER-LEVY 9 FRAGMENTS

BOSLOUGH ET AL.: NUMERICAL MODELING OF SHOEMAKER-LEVY 9 FRAGMENTS

BOSLOUGH ET AL.: NUMERICAL MODELING OF SHOEMAKER-LEVY 9 FRAGMENTS

BOSLOUGH ET AL.: NUMERICAL MODELING OF SHOEMAKER-LEVY 9 FRAGMENTS

BOSLOUGH ET AL.: NUMERICAL MODELING OF SHOEMAKER-LEVY 9 FRAGMENTS

Figure 1. Plan view (map projection) of idealized impact site from a stationary (non-rotating) vantage point, with snapshots of a planar projection of its evolution, interpreted using the conceptual framework provided by computational simulations. This figure schematically represents features that were seen after several of the larger impacts. See text for detailed explanation.

Figure 1. Plan view (map projection) of idealized impact site from a stationary (non-rotating) vantage point, with snapshots of a planar projection of its evolution, interpreted using the conceptual framework provided by computational simulations. This figure schematically represents features that were seen after several of the larger impacts. See text for detailed explanation.

Figure 2. Side view of idealized fireball/plume evolution which leads to a “hypervelocity splat” when the plume collapses, heating Jupiter’s upper atmosphere over a very large area. This highly-simplified schematic shows the ejecta cloud as a discrete packet, rather than the continuum it really is.

Figure 2. Side view of idealized fireball/plume evolution which leads to a “hypervelocity splat” when the plume collapses, heating Jupiter’s upper atmosphere over a very large area. This highly-simplified schematic shows the ejecta cloud as a discrete packet, rather than the continuum it really is.

Figure 3. Computational simulation of 3-D fireball/plume evolution after the impact of a 3-km diameter fragment. Shading indicates log(density) with a visibility cutoff at 10^{-12} g/cm^3; times are in minutes after impact.

Figure 3. Computational simulation of 3-D fireball/plume evolution after the impact of a 3-km diameter fragment. Shading indicates log(density) with a visibility cutoff at 10^{-12} g/cm^3; times are in minutes after impact.

Figure 4. Comparison of 2-D simulations demonstrating that it is the energy deposition at high altitude that controls the fireball growth. When the simulation is run using only the energy deposited from a 3-km impactor above the -50 km level (right) the fireball is almost identical to that generated by the entire energy deposition (left).

Figure 4. Comparison of 2-D simulations demonstrating that it is the energy deposition at high altitude that controls the fireball growth. When the simulation is run using only the energy deposited from a 3-km impactor above the -50 km level (right) the fireball is almost identical to that generated by the entire energy deposition (left).

TOP

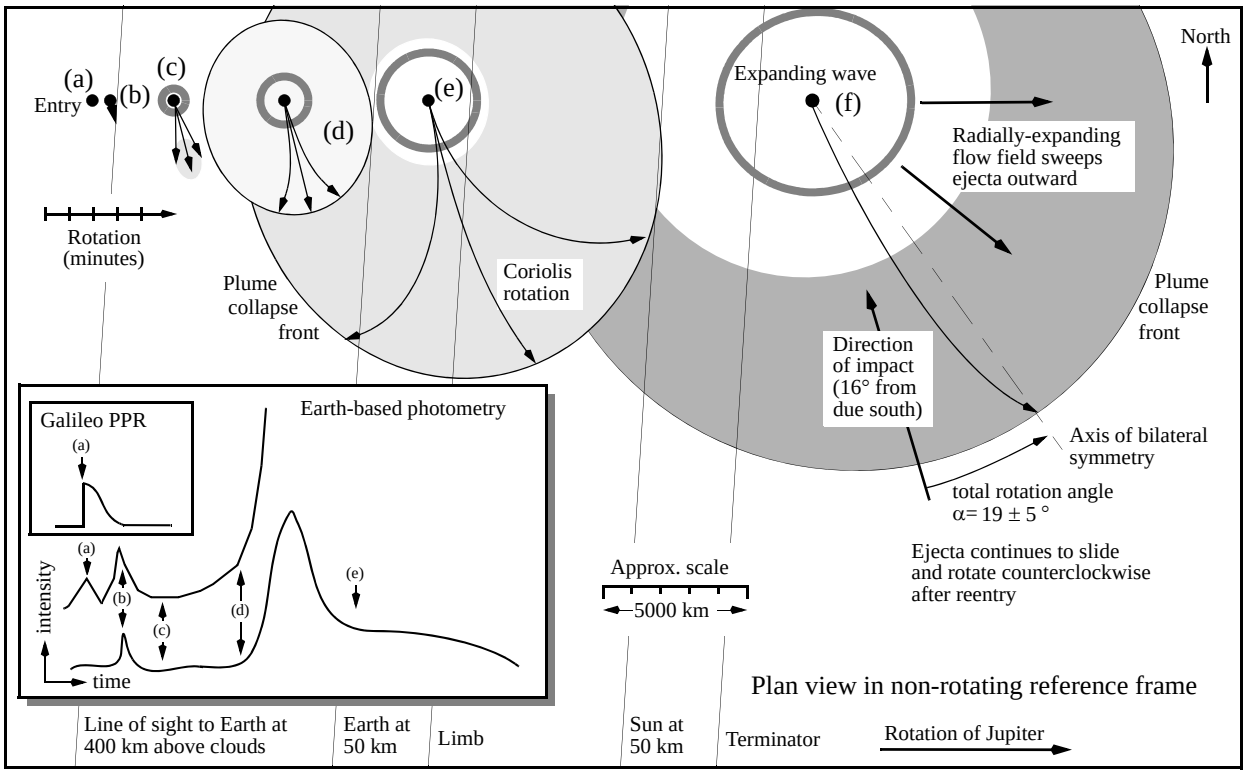
(a)
Entry
(b)
(c)
(d)
(e)
(f)
Expanding wave
North
Rotation
(minutes)
Plume
collapse
front
Coriolis
rotation
Radially-expanding
flow field sweeps
ejecta outward
Plume
collapse
front
Direction
of impact
(16° from
due south)
Axis of bilateral
symmetry
total rotation angle
α= 19 ± 5 °
Ejecta continues to slide
and rotate counterclockwise
after reentry
Galileo PPR
Earth-based photometry
intensity
time
Approx. scale
5000 km
Plan view in non-rotating reference frame
Line of sight to Earth at
400 km above clouds
Earth at
50 km
Limb
Sun at
50 km
Terminator
Rotation of Jupiter

M. B. Boslough *et al.*, Fig. 2

TOP

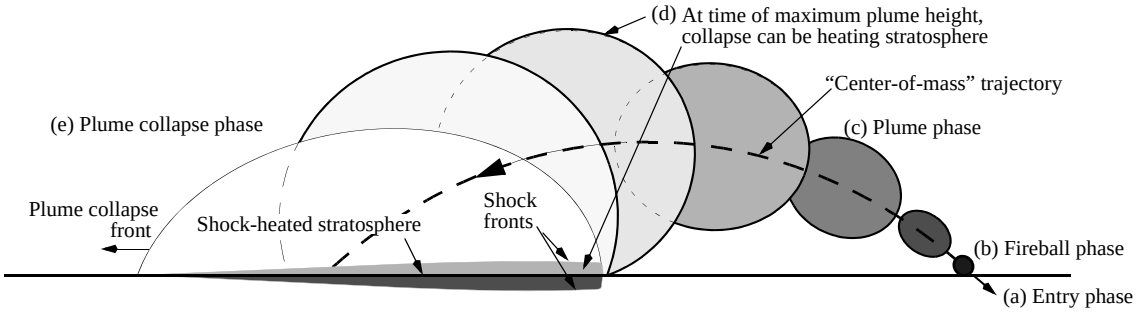

M. B. Boslough *et al.*, Fig. 3

TOP

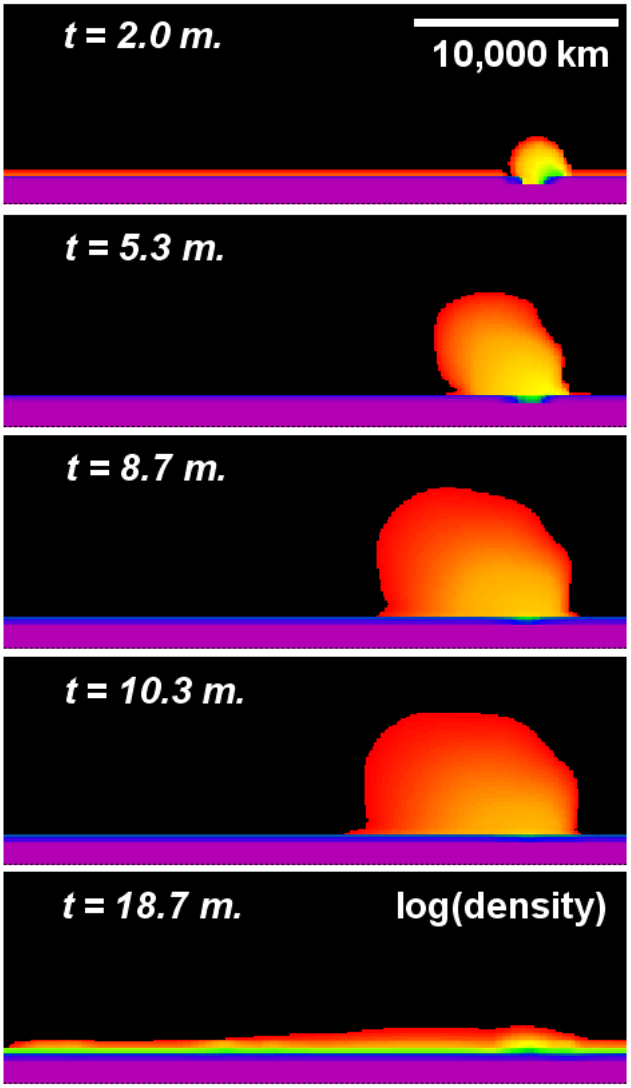

TOP